Electrophoretic deposition of donor–acceptor nanostructures on electrodes for molecular photovoltaics

Hiroshi Imahori[ab]

Received 29th June 2006, Accepted 1st September 2006
First published as an Advance Article on the web 19th September 2006
DOI: 10.1039/b609269c

Electrophoretic deposition of donor–acceptor nanostructures onto electrodes is reviewed in terms of light-to-electrical energy conversion. Various donors and acceptors and their composites have been deposited electrophoretically onto a nanostructured SnO_2 or TiO_2 electrode which exhibits photocurrent generation. In particular, bottom-up self-organization of porphyrin and fullerene molecules onto the nanostructured SnO_2 electrodes has led to highly efficient photocurrent generation with an incident photon-to-current efficiency (IPCE) of up to $\sim$60%. Such examples will give us many valuable insights into the design of organic molecular electronics including solar cells, organic transistors, and light-emitting devices.

1. Introduction

Recently, ecological considerations linked with the CO_2/global warming problem have prompted us to utilize photovoltaic solar energy. However, the present cost of electricity from silicon-based photovoltaics is much higher than the current commercial prices of electricity generated by hydraulic power or nuclear and fossil fuels. Therefore, it is necessary to develop low-cost solar cells with a high power conversion efficiency (η). Organic solar cells would be promising candidates if they fulfil these requirements.[1,2] It should be noted here that they bear unique advantages over inorganic solar cells (*i.e.*, flexibility, lightness, and colorfulness). Since the beginning of the 1990s, substantial advances in power conversion efficiency have been made in molecular photovoltaics including dye-sensitized solar cells (up to η = 7–11%)[3–6] and bulk heterojunction solar cells (up to η = 3–6%).[7–14]

[a]*Department of Molecular Engineering, Graduate School of Engineering, Kyoto University, Nishikyo-ku, Kyoto 615-8510, Japan*
[b]*Fukui Institute for Fundamental Chemistry, Kyoto University, 34-4, Takano-Nishihiraki-cho, Sakyo-ku, Kyoto 606-8103, Japan.*
E-mail: imahori@scl.kyoto-u.ac.jp

Hiroshi Imahori

Hiroshi Imahori was born in Kyoto, Japan in 1961. He completed his doctorate on organic chemistry at Kyoto University. From 1990–1992 he was a post-doctoral fellow at the Salk Institute for Biological Studies, USA. In 1992 he became an Assistant Professor at ISIR, Osaka University. In 1999 he moved to the Graduate School of Engineering, Osaka University, as an Associate Professor. Since 2002 he has been Professor of Chemistry, Graduate School of Engineering, Kyoto University.

In this context, extensive efforts have been made in recent years to explore the photovoltaic and photoelectrochemical properties of electrodes modified with various donor and acceptor components toward the realization of highly efficient organic solar cells. In the design of organic solar cells we consider the following criteria: (i) extensive light-harvesting in the visible region, (ii) efficient energy transfer to the interface of the heterojunction (if necessary) and subsequent charge separation, and (iii) efficient injection of separated electrons and holes into their respective electrodes, minimizing undesirable charge recombination. Accordingly, it is of vital importance to organize suitable donor and acceptor molecules on the electrode surface in the nanometer scale for fulfilling these requirements. Versatile methods such as Langmuir–Blodgett (LB) films,[15–22] self-assembled monolayers (SAMs),[23–47] layer-by-layer deposition,[48–59] vacuum deposition,[8,14] chemical adsorption[3–6,60,61] and spin coating[7,9,10–13,61–64] have been adopted to construct such nanostructures on electrodes for photoelectrochemical devices and solar cells.

The electrophoretic deposition technique has been widely employed, particularly in film deposition from colloidal dispersions. Electrophoretic deposition is essentially a two-step process. First, particles such as macromolecules and colloids are charged in a polar solution and forced to move toward one of two electrodes inserted into the solution by applying an electric field to the suspension. Then, the particles are deposited onto the electrode gradually, leading to the formation of an organic thin film. Thus, it is a fast and economical process which makes it possible to control nano- and micro-structures on the electrode surface. In this review article, we focus on the electrophoretic deposition method, which allows donor and acceptor molecules to be assembled onto electrodes for molecular photoelectrochemical devices. Specifically, we emphasize the utilization of porphyrins as an electron donor and fullerenes as an electron acceptor, because they exhibit small reorganization energies of electron transfer,[65–70] which makes it possible to generate a long-lived charge-separated state with a high quantum yield.

2. Electrophoretic deposition of clusters of single component

2.1 Fullerenes and other acceptors

Kamat *et al.* applied the electrophoretic deposition technique for C_{60} clusters [denoted as $(C_{60})_m$] to obtain the C_{60} films on electrodes which absorb visible light intensively and exhibit a remarkable photoelectrochemical response.[71,72] Namely, a toluene solution of C_{60} molecules is rapidly injected into acetonitrile to form C_{60} clusters with an average diameter of $\sim$300 nm due to the lyophobic nature of C_{60} in the mixed solvent (acetonitrile–toluene = 3 : 1, v/v), as illustrated in Fig. 1. Under application of a dc electric field (100–200 V), the C_{60} clusters in the mixed solvent become negatively charged and are deposited on a nanostructured SnO_2 electrode as they are driven towards the positively charged electrode surface. The broad absorption of the C_{60} film in the visible and in the near-IR region, as well as the high molar absorptivity, makes the film suitable for harvesting solar energy. Under visible light irradiation ($\lambda > 425$ nm, input power (W_{IN}) = 130 mW cm^{-2}), using I^-/I_3^- as the redox couple, the photoelectrochemical cell revealed a stable photocurrent of $\sim$0.14 mA cm^{-2} and an open circuit voltage (V_{OC}) of $\sim$0.2 V. The maximum IPCE (incident photon-to-current efficiency) of $\sim$4% was observed at the excitation wavelength of 420 nm.[71] The IPCE value is 2–3 orders of magnitude larger than previously reported values using functionalized C_{60} as photosensitizers.[15–19,23,24] Photoinduced electron transfer between iodide ions (I^-/I_3^- = 0.5 V *vs* NHE) and the excited states of C_{60} clusters ($^1C_{60}^*/C_{60}^{\bullet-}$ = 1.7 V *vs* NHE; $^3C_{60}^*/C_{60}^{\bullet-}$ = 1.4 V *vs* NHE) is the primary step in the photocurrent generation (Fig. 2). The reduced C_{60} ($C_{60}/C_{60}^{\bullet-}$ = −0.2 V *vs* NHE) then injects electrons into SnO_2 nanocrystallites (E_{CB} = 0 V *vs* NHE). The electrons transferred to the semiconductor nanocrystallites are driven to the counter electrode *via* external circuit to regenerate the redox couple.[71]

We designed two C_{60} derivatives with a phenylpyrrolidine moiety, **1** and **2**, to examine the effect of the C_{60} substituents on the structure and photoelectrochemical properties of C_{60} clusters electrophoretically deposited on nanostructured SnO_2 electrodes (Fig. 3).[73] With introducing larger substituents into C_{60}, the cluster size increases, whereas the IPCE decreases (2.3% for C_{60}, 1.1% for **1**, and 0.3% for **2** at 400 nm). The trend for photocurrent generation efficiency, as well as surface morphology on the electrode, can be rationalized by the steric

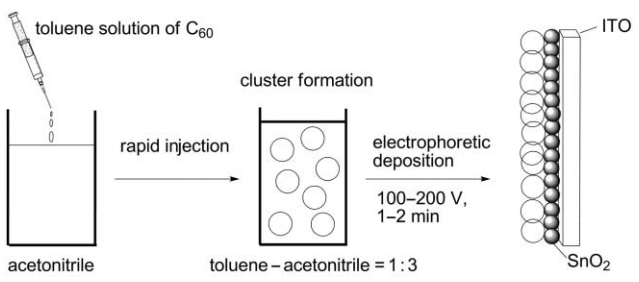

Fig. 1 Schematic illustration of cluster formation of C_{60} by rapid injection and its electrophoretic deposition onto a nanostructured SnO_2 electrode.

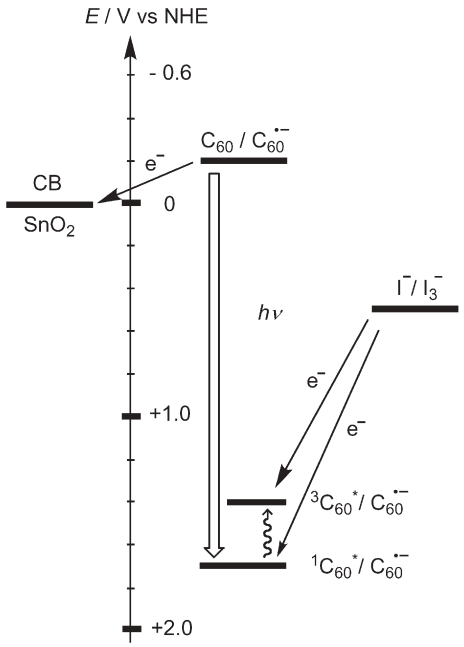

Fig. 2 Energy diagram for photocurrent generation at an ITO/SnO_2/$(C_{60})_m$ electrode.

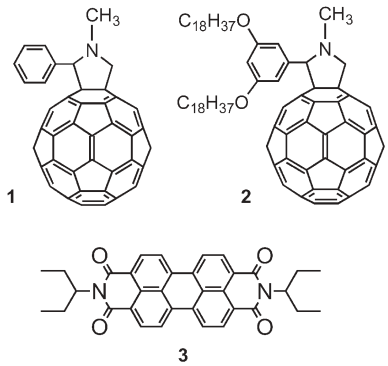

Fig. 3 Fullerene derivatives **1** and **2** and perylene diimide **3** for the cluster formation.

bulkiness around the C_{60} molecules. It is noteworthy that the C_{60} molecule with two alkoxy chains **2** is suggested to give a bilayer vesicle structure in the mixed solvent, irrespective of the hydrophobic nature of both the C_{60} and alkoxy chain moieties.[73] Such information will be valuable for the design of photoactive molecules, which are fabricated onto electrode surfaces to exhibit efficient photocurrent generation.

Kamat *et al.* assembled alkanethiol-tethered C_{60} onto a gold nanoparticle to form a photoelectrochemical device.[74] By incorporating the alkanethiol-tethered C_{60} into dodecanethiol-capped gold nanoparticles during the gold reduction step, it is possible to bind *ca.* 90 C_{60} moieties per gold nanocore. The C_{60}-modified gold nanoparticles in toluene are deposited electrophoretically onto a nanostructured SnO_2 electrode. The maximum IPCE value of 0.8% was obtained at an excitation wavelength of 450 nm.[74]

The interaction between the sensitizer and the redox couple in dye-sensitized solar cells is an important factor that controls

the power conversion efficiency.[3–6] Kamat *et al.* employed C_{60} clusters to separate ruthenium dye and I^-/I_3^- couple to minimize the undesirable sensitizer–redox couple interaction.[75] The ruthenium dye device with the C_{60} layer exhibited the maximum IPCE of 64%, which is larger by 15% than that in the ruthenium dye device without the C_{60} layer.[75]

On the other hand, it is generally difficult to find suitable conditions for forming the clusters of other acceptors in the mixed solvent to deposit them electrophoretically onto the nanostructured SnO_2 electrode. For instance, we could not deposit the clusters of perylene diimide **3** (Fig. 3) electrophoretically onto the ITO/SnO_2 electrode probably due to their small size (13 nm) in the mixed solvent.[76]

2.2 Porphyrins and phthalocyanines

Electron donors such as porphyrins and phthalocyanines can make their clusters in an acetonitrile–toluene mixture. We deposited the clusters of porphyrins and phthalocyanines electrophoretically onto the semiconducting electrodes for photoelectrochemical devices.[76,77] When a concentrated solution of 5,15-bis(3,5-di-*tert*-butylphenyl)porphyrin] **4a** (Fig. 4) in toluene is mixed with acetonitrile by fast injection method (acetonitrile–toluene = 9 : 1, v/v), the molecules aggregate and form stable clusters [denoted as $(\mathbf{4a})_m$].[77] Under application of a high dc electric field (500 V), the porphyrin clusters which become negatively charged in the mixed solvent are deposited on the nanostructured TiO_2 electrode as they are driven towards the positively charged electrode surface. Photoexcitation of the porphyrin film on the electrode in a photoelectrochemical device with visible light leads to relatively high photocurrent generation. The maximum photocurrent of 0.15 mA cm^{-2} and photovoltage of 0.25 V were attained using the I^-/I_3^- redox couple. The IPCE value of 2.0% was achieved at an applied bias potential of 0.2 V *vs* SCE. Electron injection from the porphyrin excited singlet state ($^1H_2P^*/H_2P^{\bullet+}$ = −0.7 V *vs* NHE) to the TiO_2 conduction band (E_{CB} = −0.5 V *vs* NHE) is the primary step in the photocurrent generation (Fig. 5). Then, iodide (I^-/I_3^- = 0.5 V *vs* NHE) gives electrons to the oxidized porphyrin ($H_2P/H_2P^{\bullet+}$ = 1.2 V *vs* NHE) to regenerate the redox couple.[77] The broad photoresponse of these crystallites throughout the visible range, as well as the ease of assembling them on the electrode surface, paves the way for harvesting a wide wavelength range of solar light.

Phthalocyanines **5a** (R = *n*-C_4H_9) and **5b** (R = *n*-C_8H_{17}) (Fig. 4) form optically transparent clusters in a mixture of

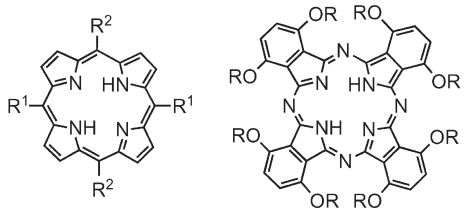

4a: R^1=3,5-(*t*-Bu)$_2C_6H_3$, R^2=H
4b: R^1=R^2=3,5-(*t*-Bu)$_2C_6H_3$

5a: R=*n*-C_4H_9
5b: R=*n*-C_8H_{17}

Fig. 4 Porphyrins **4** and phthalocyanines **5** for the cluster formation.

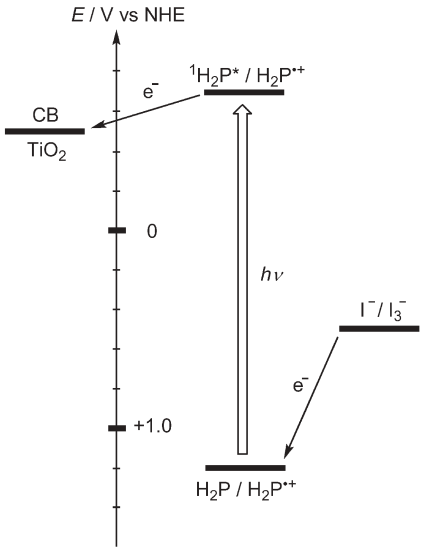

Fig. 5 Energy diagram for photocurrent generation at ITO/TiO_2/$(\mathbf{4a})_m$ electrode.

toluene–acetonitrile after rapid injection of the toluene solution into acetonitrile [denoted as $(\mathbf{5})_m$].[76] The clusters of **5b** in the toluene–acetonitrile mixture exhibit a structureless broad absorption in the 300–500 and 700–800 nm range with lower molar coefficients, compared to the monomeric form in toluene. These results confirm that the phthalocyanine molecules aggregate and form clusters in the mixed solvents as in the case of porphyrins and/or fullerenes. In contrast, phthalocyanine **5a** does not reveal such a spectral change under the same conditions. This suggests that the long alkyl chains of **5b** relative to those of **5a** have a large impact on the formation of clusters in the mixed solvents. Under application of a high dc electric field (250 V for 2 min), the clusters $(\mathbf{5b})_m$, which are positively charged in the toluene–acetonitrile, are driven towards the negatively charged electrode surface [denoted as ITO/SnO_2/$(\mathbf{5b})_m$].[76] This behavior is in sharp contrast with porphyrins and fullerenes in which they are negatively charged under application of a dc voltage, leading to deposition on the positively charged electrode (*vide supra*). Photoelectrochemical measurements were performed under the standard three electrode system (0.15 V *vs* SCE). The IPCE value of the phthalocyanine photoelectrochemical device (0.1–1%)[76] is rather smaller than those of the porphyrin devices using **4a** (~2.0%)[77,78] and **4b** (~1%) (*vide infra*).[79] In the case of the porphyrins, bulky *t*-butyl groups are introduced into the *meta* positions of the *meso*-phenyl groups of the porphyrins to avoid the undesirable aggregation that leads to the self-quenching of the porphyrin excited singlet state. On the other hand, the present phthalocyanine **5b** possesses relatively long alkoxy chains which induce π–π stacking of the phthalocyanine rings, resulting in the relatively strong self-quenching of the excited singlet state. Such difference in the photophysics of the phthalocyanine and the porphyrins may be responsible for the difference in the IPCE values. This matches the strong tendency of phthalocyanines to aggregate on the nanostructured SnO_2 or TiO_2 electrodes, leading to low IPCE of phthalocyanine-sensitized solar cells (<4%).[76]

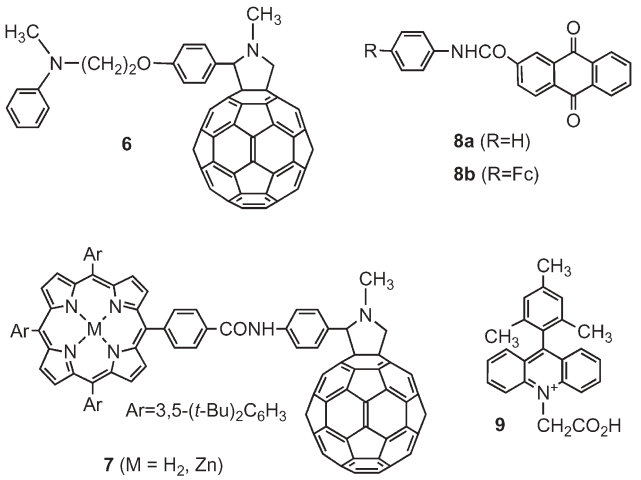

Fig. 6 Donor–acceptor linked molecules **6**–**9** for the cluster formation.

3. Electrophoretic deposition of clusters of donor and acceptor composites

3.1. Donor–acceptor linked systems

Kamat *et al.* deposited clusters of C_{60}-aniline linked dyad **6** as thin films on a nanostructured SnO_2 electrode under the influence of an electric field (Fig. 6).[80] Photoelectrochemical measurements were carried out under the standard two electrode arrangement. The maximum IPCE of ~4% is noted at 450 nm,[80] which is comparable to that (~4%) of similar photoelectrochemical device with C_{60} itself.[71] Thus, there is no substantial effect of C_{60} as an electron mediator on photocurrent enhancement in this system.

In a collaboration with Kamat *et al.*, we applied the electrophoretic deposition method to porphyrin–fullerene linked dyads **7** (M = H_2, Zn) to assemble the dyad clusters on a nanostructured SnO_2 electrode (Fig. 6).[81] The cluster films of **7**, when electrophoretically deposited on the nanostructured SnO_2 electrodes, are photoactive and generate anodic photocurrent under standard three electrode arrangement (0 V *vs* Ag/AgCl) [denoted as ITO/SnO_2/(**7**)$_m$/LiI + I_2/Pt device]. Although the light-harvesting efficiency (maximal absorbance = 1.6) is improved by a factor of 11 compared to the monolayer system (~0.04), the maximum IPCE values are found to be still low (0.36% for ITO/SnO_2/(**7**(M = H_2))$_m$/LiI + I_2/Pt device and 0.42% for ITO/SnO_2/(**7**(M = Zn))$_m$/LiI + I_2/Pt device).[81] The maximum IPCE values are smaller than those of photoelectrochemical devices (~9%) in which a similar porphyrin–C_{60} dyad is physically adsorbed onto a SnO_2 electrode.[60] Although such donor–acceptor linked molecules are designed to exhibit a long-lived charge-separated state with a high quantum yield in solutions,[65–70] the linkage between the donor and the acceptor would not be optimized for the desirable molecular packing of the dyads in the thin film, so that separated hole and electron are not injected efficiently into the respective electrodes.

Fukuzumi and Kamat *et al.* employed formanilide–anthraquinone dyad **8a** and ferrocene (Fc)–formanilide–anthraquinone dyad **8b** (Fig. 6) as components of photoelectrochemical devices where composite clusters of **8a** or **8b** with C_{60} are assembled onto a SnO_2 electrode using the electrophoretic deposition method.[82] Photocurrent measurements were performed under the standard three electrode arrangement [denoted as ITO/SnO_2/(**8a** + C_{60})$_m$ or (**8b** + C_{60})$_m$/NaI + I_2/Pt device]. The maximum IPCE value (9.7% at 470 nm) in ITO/SnO_2/(**8a** + C_{60})$_m$/NaI + I_2/Pt device is 10 times as large as that (0.98% at 465 nm) in ITO/SnO_2/(**8b** + C_{60})$_m$/NaI + I_2/Pt device (0 V *vs* SCE). Such enhancement in photocurrent generation can be ascribed to the dramatic difference in the lifetimes of the charge-separated states of **8a** (900 μs) and **8b** (20 ps) in DMSO.[82]

Fukuzumi and Imahori *et al.* reported photovoltaic cell comprising of 9-mesityl-10-carboxymethylacridinium ion **9** and C_{60} clusters (Fig. 6).[83] 9-Mesityl-10-carboxymethylacridinium ion **9** is adsorbed chemically onto a SnO_2 electrode, followed by the electrophoretic deposition of the C_{60} cluster onto the SnO_2 electrode. Photoelectrochemical measurements were performed using the standard three electrode system [denoted as ITO/SnO_2/**9** + (C_{60})$_m$/NaI + I_2/Pt device]. The IPCE value in ITO/SnO_2/**9** + (C_{60})$_m$/NaI + I_2/Pt device reaches 25% at 480 nm at an applied potential of 0.2 V *vs* SCE, whereas the maximum IPCE value of ITO/SnO_2/**9**/NaI + I_2/Pt device is 2% at 460 nm.[83]

Fukuzumi and Kamat *et al.* deposited electrophoretically the composite clusters of C_{60} and TiO_2 nanoparticles modified with **9** (TiO_2–**9**) in acetonitrile–toluene (3 : 1, v/v) onto a nanostructured SnO_2 electrode.[84] The TiO_2 nanoparticles act as scaffold to organize **9** and C_{60}. The IPCE value in ITO/SnO_2/(TiO_2–**9** + C_{60})$_m$/NaI + I_2/Pt device reaches 37% at 480 nm at an applied potential of 0.2 V *vs* SCE, whereas the maximum IPCE value of ITO/SnO_2/(TiO_2–**9**)$_m$/NaI + I_2/Pt device is 5% at 480 nm.[84] Although **9** is reported to exhibit an extremely long-lived charge-separated state with a high quantum yield,[85] C_{60} as an electron mediator between the charge-separated state and the SnO_2 electrode is necessary to achieve efficient photocurrent generation.

3.2. Donor and acceptor composite systems

Composites of donor and acceptor in the form of clusters have been assembled as three-dimensional network on an electrode surface for attaining efficient photocurrent generation. Kamat *et al.* prepared composite clusters of various donors (*N*,*N*-dimethylaniline, *N*,*N*-dimethyl-*p*-toluidine, ferrocene, *N*-methylphenothiazine, and *N*,*N*-dimethyl-*p*-anisidine) and 1,2,5-triphenylpyrrolidinofullerene which are deposited electrophoretically onto a nanostructured SnO_2 electrode.[86] The maximum IPCE of ~0.05% is obtained at 420 nm,[86] which is much smaller than those of a similar photoelectrochemical device with C_{60} (1.6–4% at 420 nm)[71] and fullerene derivatives (0.2–0.8% at 400 nm).[73]

In a collaboration with Kamat *et al.*, we applied bottom-up self-assembly to porphyrin and fullerene single components and the composites to construct a novel organic solar cell (dye-sensitized bulk heterojuntion solar cell), possessing both the dye-sensitized and bulk heterojunction characteristics.[78,87,88] We have already found, for the first time, that there is π–π interaction between porphyrin and fullerene in the ground and

excited states.[89–93] The specific interaction between porphyrin and fullerene is suitable for electrophoretic deposition of the composite clusters. Bearing this in mind, we make a supramolecular complex of porphyrin and fullerene in toluene due to the π–π interaction (step 1).[78,87,88] Then, the supramolecular complex is self-assembled into larger clusters in a mixture of toluene and acetonitrile due to lyophobic interaction between the complex and the mixed solvent (step 2). Finally, the larger clusters can be further associated onto a nanostructured SnO_2 electrode using the electrophoretic deposition technique (step 3).

The electrophoretic deposition method is adopted to prepare a film of the composite clusters of porphyrin **4a** and C_{60} [denoted as (**4a** + C_{60})$_m$] on an ITO/SnO_2 electrode.[78] Photocurrent measurements were performed under the standard two electrode system [denoted as ITO/SnO_2/(**4a** + C_{60})$_m$/NaI + I_2/Pt device]. The short circuit photocurrent density (J_{SC}) of 0.18 μA cm^{-2}, open circuit voltage (V_{OC}) of 0.21 V, fill factor (*ff*) of 0.35, and η of 0.012% (input power (W_{IN}) = 110 mW cm^{-2}) are obtained for ITO/SnO_2/(**4a** + C_{60})$_m$/NaI + I_2/Pt device. The maximum IPCE value of 4.5% at 430 nm for ITO/SnO_2/(**4a** + C_{60})$_m$/NaI + I_2/Pt device is larger than the sum (~2%) of the IPCE value (0.6%) for ITO/SnO_2/(**4a**)$_m$/NaI + I_2/Pt and that (1.6%) for ITO/SnO_2/(C_{60})$_m$/NaI + I_2/Pt reference devices. Note that the maximum IPCE value of 17% is obtained at 460 nm for ITO/SnO_2/(**4a** + C_{60})$_m$/NaI + I_2/Pt device at an applied potential of 0.2 V *vs* SCE. Such enhancement in the photocurrent generation of the composite cluster devices from **4a** and C_{60} demonstrates that charge separation between the excited porphyrin and C_{60} in the supramolecular complex is a dominating factor for efficient photocurrent generation. Namely, ultrafast photoinduced electron transfer occurs from the porphyrin singlet excited state ($^1H_2P^*/H_2P^{\bullet+}$ = −0.7 V *vs* NHE) to C_{60} ($C_{60}/C_{60}^{\bullet-}$ = −0.2 V *vs* NHE) in the complex. The reduced C_{60} transfers electrons to the conduction band of SnO_2 nanocrystallites (E_{CB} = 0 V *vs* NHE) by electron hopping through large excess of C_{60} molecules. The regeneration of H_2P clusters ($H_2P/H_2P^{\bullet+}$ = 1.2 V *vs* NHE) is achieved by the iodide/triiodide couple (I^-/I_3^- = 0.5 V *vs* NHE) present in the electrolyte system (Fig. 7).[78]

The present organic solar cell, "dye-sensitized bulk heterojunction solar cell," is unique in that it possesses both characteristics of dye-sensitized and bulk heterojunction solar cells. Namely, initial charge separation occurs at the interface of the donor and the acceptor, which is typical characteristic of bulk heterojunction solar cells. Nevertheless, the following other processes are similar to those in dye-sensitized solar cells. It is noteworthy that the composite film reveals the multilayer structure on ITO/SnO_2, which presents a striking contrast to monolayer structure of adsorbed dyes on TiO_2 electrodes in dye-sensitized solar cells. Therefore, we can expect improvement of the photovoltaic properties by modulating both the structures of electrode surfaces and donor–acceptor multilayers.

A drawback of the electrophoretic deposition of donor–acceptor composites is the difficulty of codeposition of positively charged donors and negatively charged acceptors or *vice versa*, which are electrophoretically deposited onto

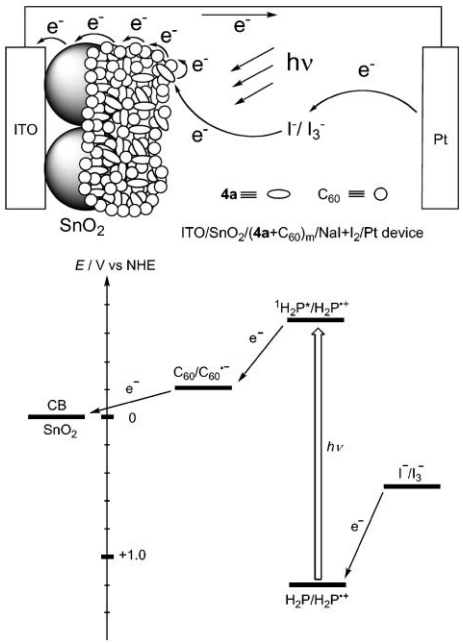

Fig. 7 Schematic photocurrent generation and energy diagram in dye-sensitized bulk heterojunction solar cells consisting of **4a** and C_{60}.

respective electrodes. For instance, under application of a high dc electric field, the clusters of C_{60} and C_{60} derivatives, which tend to be negatively charged in toluene–acetonitrile, are driven towards the positively charged electrode surface. On the other hand, the clusters of phthalocyanines, which tend to be positively charged in toluene–acetonitrile, are driven toward the negatively charged electrode surface. Thus, the composite clusters of phthalocyanine and C_{60} cannot be deposited onto the same electrode. Nevertheless, the composite clusters of phthalocyanine **5b** and perylene diimide **3** [denoted as (**5b** + **3**)$_m$] can be attached onto ITO/SnO_2 electrodes by the electrophoretic deposition [denoted as ITO/SnO_2/(**5b** + **3**)$_m$].[76] Under application of a high dc electric field (250 V for 2 min), the clusters (**5b** + **3**)$_m$ (which are positively charged in toluene–acetonitrile) are driven towards the negatively charged electrode surface. Although the IPCE value of the ITO/SnO_2/(**5b** + **3**)$_m$ device (<1%)[76] is rather low compared to similar porphyrin systems,[77–79] the enhancement of the photocurrent generation efficiency of the composite system is achieved relative to the phthalocyanine reference system without the perylene diimide. This is an example for dye-sensitized bulk heterojunction solar cells using different combination of donor and acceptor (*i.e.*, phthalocyanine and perylene diimide).[76]

3.3. Pre-organized porphyrin systems

Supramolecular assembly of donor–acceptor molecules is a potential approach to create a desirable phase-separated, interpenetrating network involving molecular-based nanostructured electron and hole highways in the blend films of donor and acceptor for bulk heterojunction solar cells. However, different, complex hierarchies of self-organization going from simple molecules to devices have limited improvement of the device performance. To construct such complex

hierarchies comprising of donor and acceptor molecules on electrode surfaces, pre-organized molecular systems are excellent candidates for achieving the molecular architectures. In particular, porphyrins have been three-dimensionally organized using dendrimers,[79,94] oligomers,[95] and nano- and micro- particles[96–104] as nanoscaffold to combine with fullerenes for organic solar cells.

3.3.1 Multiporphyrin dendrimers. The collaborative efforts of Imahori, Fukuzumi, Kamat, and Crossley *et al.* have continued to develop the novel light energy conversion system using supramolecular complexes of multiporphyrin dendrimers (Fig. 8) with C_{60} by clusterization in the acetonitrile–toluene mixed solvent and electrophoretic deposition onto a nanostructured SnO_2 electrode.[79,94] First, porphyrin molecules are attached at the terminals of each dendritic branch to yield multiporphyrin dendrimers (**10**(*n*): *n* = number of the porphyrins in **10**, step 1). Second, C_{60} molecules are incorporated into **10** in toluene due to the π–π interaction (step 2). Then, the resulting supramolecular complexes of **10** and C_{60} are further associated to become larger clusters in the mixed solvent due to the lyophobic interaction (step 3). Finally, the composite clusters are deposited on the nanostructured SnO_2 electrode by the electrophoretic deposition method (step 4). Upon subjecting the resultant cluster suspension to a high electric DC field, the composite clusters of **10** and C_{60} [denoted as (**10** + C_{60})$_m$] and of porphyrin reference **4b** and C_{60} [denoted as (**4b** + C_{60})$_m$] are deposited onto the ITO/SnO_2 electrode to give modified electrodes [denoted as ITO/SnO_2/(**10** (*n*) + C_{60})$_m$(*n* = 4,8,16) and ITO/SnO_2/(**4b** + C_{60})$_m$, respectively]. Photoelectrochemical measurements were performed with the standard two electrode system [denoted as ITO/SnO_2/(**10**(*n*) + C_{60})$_m$/NaI + I_2/Pt device]. It is noteworthy that the IPCE value of ITO/SnO_2/(**10**(*n*) + C_{60})$_m$/NaI + I_2/Pt(*n* = 4, 8, 16) device decreases with increasing the dendritic generation. Such a trend may result from the rigid structures of the porphyrin moieties in the higher generation, which inhibits the efficient incorporation of C_{60} molecules between the porphyrins in **10**. The ITO/SnO_2/(**10**(4) + C_{60})$_m$/NaI + I_2/Pt device has *ff* of 0.31, V_{OC} of 0.22 V, J_{SC} of 0.29 mA cm^{-2}, and η of 0.32% at W_{IN} of 6.2 mW cm^{-2}. The η value of ITO/SnO_2/(**10**(4) + C_{60})$_m$/NaI + I_2/Pt device is 10 times as large as that of the ITO/SnO_2/(**4b** + C_{60})$_m$/NaI + I_2/Pt reference device (η = 0.035%).[79,94]

3.3.2. Porphyrin oligomers. Fukuzumi, Kamat, and Solladié *et al.* presented organic photovoltaic cells using supramolecular complexes of porphyrin–peptide oligomers **11** (*n* = 1,2,4,8) with C_{60} (Fig. 9).[95] The SnO_2 electrodes modified with the composite clusters of **11** with C_{60} are prepared as in the case of **10** and C_{60} composite system. Photoelectrochemical measurements were performed with the standard two electrode system [denoted as ITO/SnO_2/(**11** + C_{60})$_m$/NaI + I_2/Pt device]. The η value of 1.3% (*ff* = 0.47, V_{OC} = 0.30 V, W_{IN} = 3.4 mW cm^{-2}) and IPCE of 42% at 600 nm are attained using the composite clusters of porphyrin peptide octamer and C_{60} in the ITO/SnO_2/(**11**(*n* = 8) + C_{60})$_m$/NaI + I_2/Pt device. The η value (1.3%) of ITO/SnO_2/(**11**(*n* = 8) + C_{60})$_m$/NaI + I_2/Pt device is 30 times as large as that (0.043%) of ITO/SnO_2/(**11**(*n* = 1) + C_{60})$_m$/NaI + I_2/Pt device. These results clearly show that the formation of a molecular assembly between C_{60} and multi-porphyrin arrays with a polypeptide backbone as

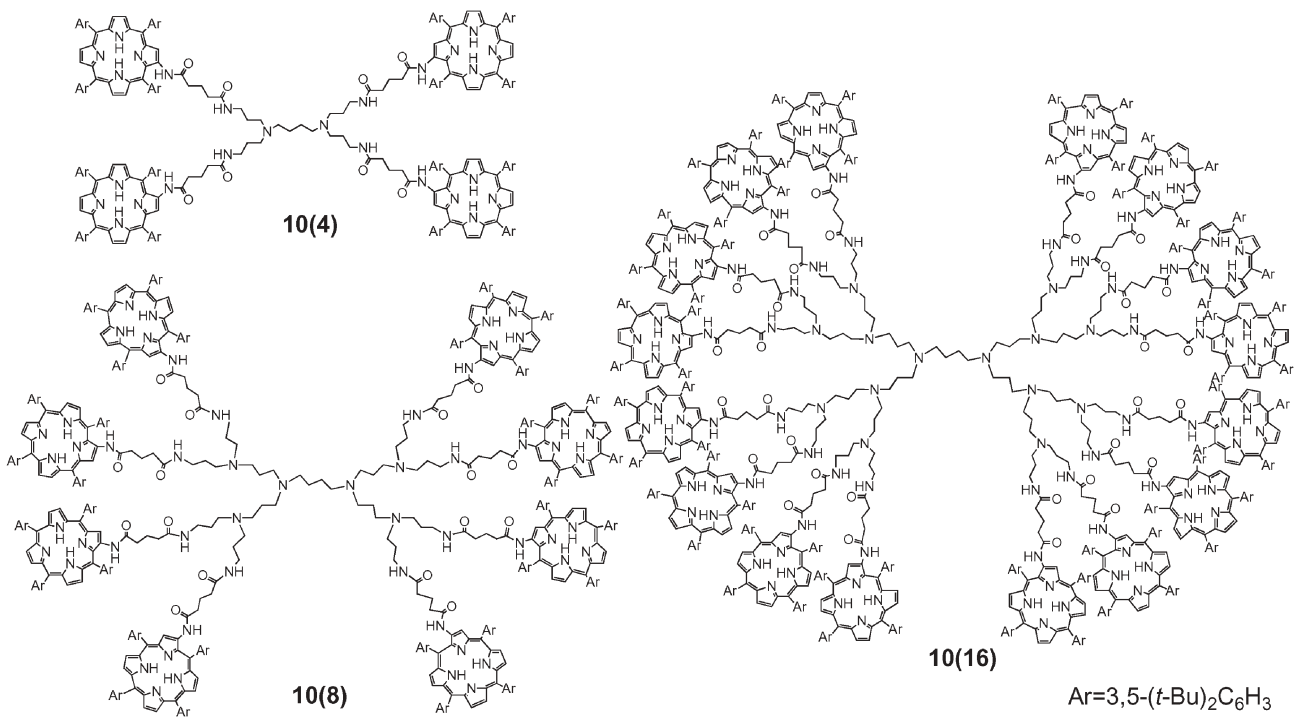

Fig. 8 Molecular structures of multiporphyrin dendrimers **10** (*n*) (*n*: number of the porphyrins in the dendrimer (*n* = 4, 8, 16)) for dye-sensitized bulk heterojunction solar cells.

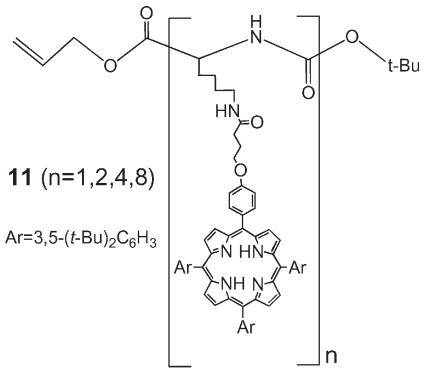

Fig. 9 Molecular structures of porphyrin oligomers **11** (n = 1, 2, 4, 8) for dye-sensitized bulk heterojunction solar cells.

nanoscaffold modulates the electron transfer efficiency in the supramolecular complex, which is essential for the efficient light-energy conversion.[95]

3.3.3. Multiporphyrin-modified nanoparticles. We extend the concept of dye-sensitized bulk heterojunction solar cells into more sophisticated supramolecular systems prepared using bottom-up self-organization of porphyrin and fullerene with gold nanoparticles on a SnO_2 electrode as shown in Fig. 10.[96,97] First, porphyrin–alkanethiol molecules **12** (n: number of the methylene groups in the alkanethiol; n = 5, 11, 15)[105,106] are three-dimensionally organized onto a gold nanoparticle with a diameter of ~2 nm to give multiporphyrin-modified gold nanoparticles **13** (n = 5, 11, 15) with well-defined size (~10 nm) and spherical shape (step 1). These nanoparticles bear flexible host space between the porphyrins for guest molecules (*i.e.*, C_{60}). Thus, the nanoparticles **13** incorporate C_{60} molecules between the porphyrin moieties due to the π–π interaction (step 2). Then, the resultant supramolecular complexes are grown into larger clusters with a size of ~100 nm in the acetonitrile–toluene mixed solvent due to the lyophobic interaction (step 3). Finally, the large clusters are deposited electrophoretically onto the SnO_2 electrode (step 4). Photoelectrochemical measurements were performed with the standard two electrode system [denoted as ITO/SnO_2/(**13** + $C_{60})_m$/NaI + I_2/Pt device]. The IPCE value of ITO/SnO_2/(**13** + $C_{60})_m$/NaI + I_2/Pt device (up to 54% (n = 15)) increases with increasing the chain length (n = 5, 11, 15) between the porphyrin and the gold nanoparticle. The long methylene spacer of **13** allows suitable space for C_{60} molecules to accommodate them between the neighboring two porphyrin rings effectively relative to the clusters with the short methylene spacer, leading to more efficient photocurrent generation. On the other hand, further increase of spacer length between the porphyrin and the gold nanoparticle results in a rather decrease of the IPCE value.[98] Additionally, replacement of C_{60} with C_{70} or free base porphyrin with zinc porphyrin leads to a decrease of the photoelectrochemical response. The preference may be explained by the difference in the complexation abilities between the porphyrin and fullerene molecules as well as in the electron or hole hopping efficiency in the composite clusters. The ITO/SnO_2/(**13**(n = 15) + $C_{60})_m$/NaI + I_2/Pt device has *ff* of 0.43, V_{OC} of 0.38 V, J_{SC} of 1.0 mA cm^{-2}, and η of 1.5% at W_{IN} of 11.2 mW cm^{-2}. The *I*–*V* characteristics of ITO/SnO_2/(**13**(n = 15) + $C_{60})_m$/NaI + I_2/Pt device is also remarkably enhanced by a factor of 45 in comparison with ITO/SnO_2/(**4b** + $C_{60})_m$/NaI + I_2/Pt device. These results clearly show that the large improvement of the

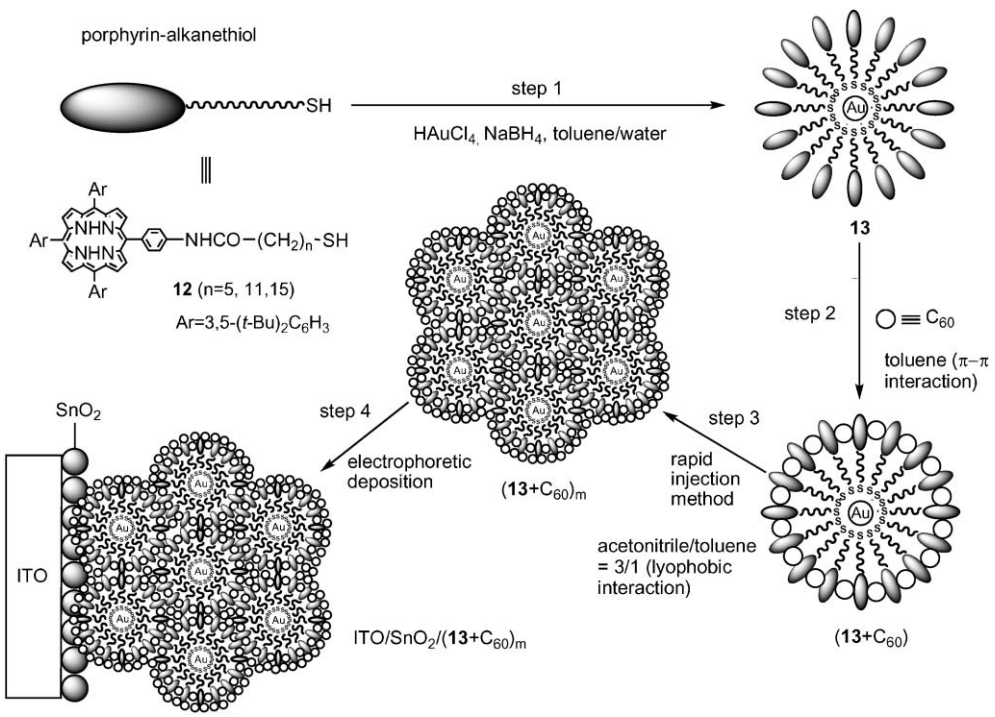

Fig. 10 Schematic diagram for step-by-step organization of porphyrin–alkanethiol **12** and C_{60} onto a nanostructured ITO/SnO_2 electrode *via* porphyrin-modified gold nanoparticle **13** (n = 5, 11, 15).

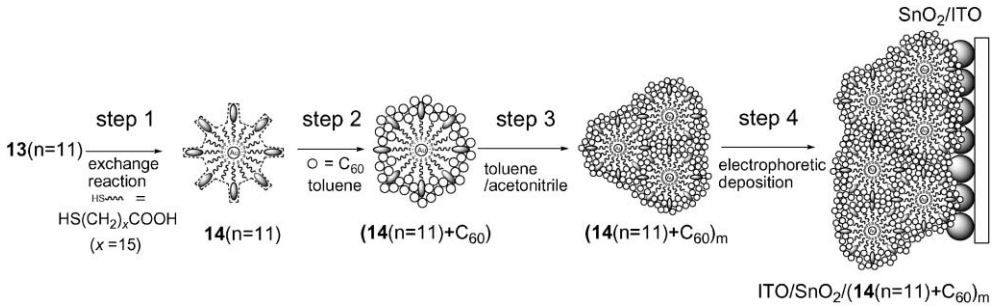

Fig. 11 Schematic diagram for step-by-step organization of porphyrin-modified gold nanoparticle **13** (n = 11) and C_{60} onto a nanostructured ITO/SnO_2 electrode *via* porphyrin-modified gold nanoparticle **14** (n = 11) with a large, bucket-shaped hole on the surface for the binding of C_{60}.

photoelectrochemical properties results from three-dimensional interpenetrating network of the porphyrin and C_{60} molecules on the nanostructured SnO_2 electrode which facilitates the injection of the separated electron into the conduction band.[96,97]

We further continued this novel approach to construct a light energy conversion system using the supramolecular incorporation of C_{60} molecules (guest) into tailored, large and bucket-shaped surface holes (host) on porphyrin-modified gold nanoparticles **14** in the mixed solvent, followed by the electrophoretic deposition on a nanostructured SnO_2 electrode (Fig. 11).[99,100] First, some of porphyrin molecules on a gold nanoparticle **13** (n = 11) are exchanged with short alkanethiol molecules to yield **14** (n = 11) with large and bucket-shaped surface holes (step 1). The SnO_2 electrodes modified with the composite clusters of **14** (n = 11) with C_{60} are prepared as in the case of **13** and C_{60} composite system. The difference in the porphyrin–C_{60} ratio is found to affect the structures and photoelectrochemical properties of the composite clusters in the mixed solvents as well as on the SnO_2 electrodes. Photoelectrochemical measurements were performed with the standard three electrodes system [denoted as ITO/SnO_2/(**14**(n = 11) + $C_{60})_m$/LiI + I_2/Pt device]. The maximum IPCE value (42%) of ITO/SnO_2/(**14**(n = 11) + $C_{60})_m$/LiI + I_2/Pt device with large, bucket-shaped holes is larger by a factor of 3 than that (16%) of ITO/SnO_2/(**13**(n = 11) + $C_{60})_m$/LiI + I_2/Pt device with small, wedge-shaped surface holes on **13** (n = 11) at an applied potential of +0.06 V *vs* SCE. This clearly demonstrates that the shape and size of the host holes on the three-dimensional porphyrin-modified gold nanoparticles have a large impact on the photoelectrochemical properties. Remarkable enhancement in the photoelectrochemical performance as well as broader photoresponse in the visible and infrared relative to the reference systems demonstrates that the bottom-up self-organization approach provides a novel perspective for the development of efficient organic solar cells.[99,100]

The drawbacks of utilizing gold nanoparticles as nanoscaffolds are their expensive cost and the relatively strong energy transfer quenching of the porphyrin excited singlet state by the gold surface. Thus, inexpensive nanoparticles as a scaffold of porphyrin molecules without such energy transfer quenching would be required to improve photocurrent generation efficiency in the composite cluster systems with C_{60}. Silica nanoparticles are potential candidates because of their low cost, non-photoactive characteristics, and facile functionalization. A silica micro- and nano-particle **15** has been successfully employed as a scaffold to self-organize porphyrin and C_{60} molecules on a nanostructured SnO_2 electrode (Fig. 12).[101,102] The quenching of the porphyrin excited singlet state on the silica nanoparticle is suppressed significantly, showing that silica nanoparticles are promising scaffolds for organizing photoactive molecules three-dimensionally in nanometer scale. Marked enhancement of the photocurrent generation (10–17%) was achieved in the porphyrin-modified silica particle devices with C_{60} compared to the reference device (4% for **13** (n = 5)) with a similar length of spacer between the porphyrin and the particle in which gold core was employed as a scaffold of porphyrins instead of silica particles. The rather small IPCE value (10%) of the silica nanoparticle device relative to that using silica microparticles (17%) may result from poor electron and hole mobility in the composite film due to poor connection between the composite clusters of porphyrin-modified silica nanoparticle and C_{60} in micrometer scale.[101,102]

3.3.4. Preprogrammed donor and acceptor composites. The bottom-up self-assembled film of the composite clusters exhibited an IPCE value of up to 54%. However, preparation of such three-dimensionally pre-organized molecules is generally difficult and unlikely to be realistic for the possible future applications. Therefore, it is highly desirable to exploit a supramolecular photoelectrochemical device consisting of

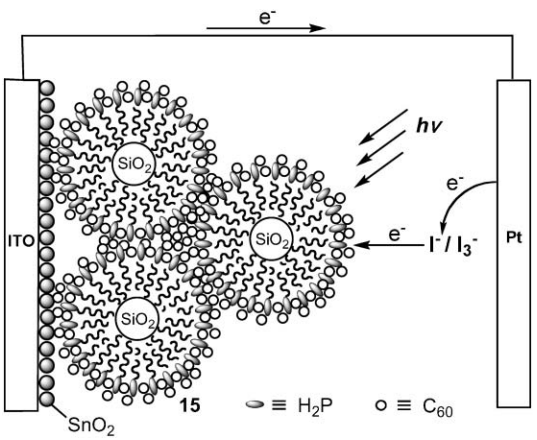

Fig. 12 Schematic photocurrent generation at a nanostructured ITO/SnO_2 electrode electrophoretically deposited with composite clusters of porphyrin-modified silica particle **15** and C_{60}.

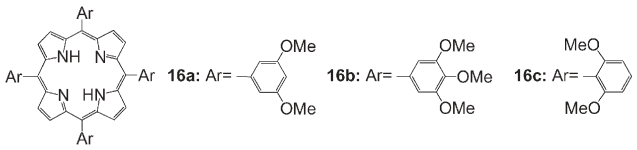

Fig. 13 Molecular structures of self-assembling porphyrins **16** used in this study.

preprogrammed self-assembling porphyrin and C_{60} single component composites, which exhibit efficient photocurrent generation as a result of segregated nanoarrays of porphyrin and fullerene on SnO_2 electrodes.

We examined the substituent effect of *meso*-tetraphenylporphyrin **16** on the nanostructure and photoelectrochemical properties of SnO_2 electrodes modified electrophoretically with the composite clusters of **16** and C_{60} (Fig. 13).[107] To facilitate the supramolecular complexation between the porphyrin and C_{60}, electron-donating substituents (*i.e.*, methoxy group) are introduced into the 3,5-positions (**16a**), 3,4,5-positions (**16b**), and 2,6-positions (**16c**) of the *meso*-phenyl groups at the porphyrin ring. The maximum IPCE value (59% at 425 nm) of ITO/SnO_2/(**16a** + C_{60})$_m$ device is much larger than those of ITO/SnO_2/(**16b** + C_{60})$_m$ (10%), ITO/SnO_2/(**16c** + C_{60})$_m$ (5.7%), and other related porphyrin and C_{60} single component composite devices (1–17%).[78,79] It should be emphasized here that the simple substituent of methoxy groups onto the *meta*-positions of the *meso*-phenyl groups at the porphyrin ring is responsible for the efficient photocurrent generation, which is much superior to the systems from the more complex, time-consuming pre-organized porphyrin molecular assemblies and C_{60}.[94–104] Various spectroscopic and surface analyses revealed that the molecular arrangement of **16a** and C_{60} composite clusters on the SnO_2 electrode involves a similar specific molecular packing of single crystal **16a**·2C_{60}·toluene in which the porphyrin and C_{60} make an alternative layer structure where the closest porphyrin moieties (center-to-center distance (R_{cc}) = 14.2 Å) are arranged in a one-dimensional chain with a dihedral angle of 66°, while the closest C_{60} moieties (R_{cc} = 10.2 Å) in a two-dimensional sheet with sandwiching **16a** between two C_{60} molecules (Fig. 14). The segregated nanoarrays of porphyrin and fullerene on the SnO_2 electrode allow the system to undergo ultrafast electron transfer or charge transfer (<100 fs) between the supramolecular complex of the porphyrin and C_{60} molecules, followed by hole and electron relay through the nanostructured one-dimensional porphyrin chains and two-dimensional C_{60} sheets, leading to efficient photocurrent generation.[107] In bulk heterojunction solar cells, many researchers have suggested the importance of nanostructured electron and hole transporting highways which have never been confirmed experimentally.[1,7–14] Our finding is the first experimental demonstration for this hypothesis. Such results provide many valuable insights into the design of molecular photovoltaics in the nanoscale.

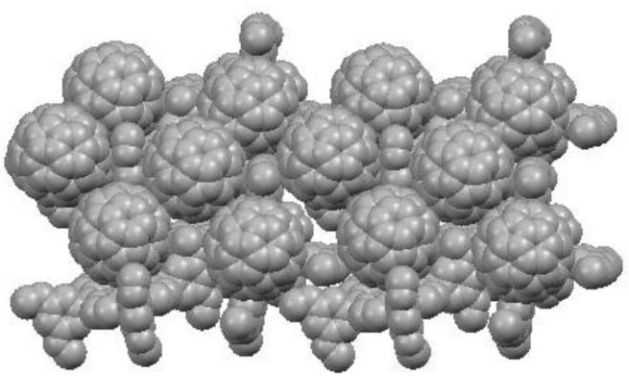

Fig. 14 Molecular packing of **16a**·(C_{60})$_2$·(toluene). Parts of the C_{60} and toluene molecules are omitted for clarity.

4. Summary

This review article has focused on recent advances in electrophoretic deposition for photoelectrochemical devices and organic solar cells. Electron transfer reactions between donors and acceptors have been well understood on the basis of electron transfer parameters including the driving force, electronic coupling matrix elements, reorganization energy, and temperature, in the light of Marcus theory of electron transfer. In the next stage, chemists must apply such principle to donor–acceptor assemblies in a solid-state which exhibits specific functions of interest. However, it is still difficult to predict molecular packing of the solid-state donor–acceptor composites and its resultant function from the molecular structures of the donor and acceptor. Recent advances in electrophoretic deposition of donor–acceptor nanostructures on electrodes will give us a deep insight into the design of molecular devices. In such cases, utilization of weak intermolecular interactions between donor–donor, acceptor–acceptor, and donor–acceptor for forming the nanostructures on the electrode plays a key role in the construction of organic molecular electronics such as organic transistors, solar cells, and light-emitting devices. Preprogrammed, self-assembling simple molecules will allow us to achieve such functions without difficulty in terms of synthesis and fabrication. Moreover, the search for novel and better nanomaterials such as carbon nanotubes[108,109] and nanoparticles[110] should continue to combine with electrophoretic deposition methods for the development of organic molecular electronics.

Acknowledgements

The authors are deeply indebted to the work of all collaborators and co-workers whose names are listed in the references (in particular, Prof. S. Fukuzumi, Prof. H. Lemmetyinen, Prof. N. V. Tkachenko, Prof. P. V. Kamat, and Prof. M. Crossley). H. I. thanks Grants-in-Aid from MEXT, Japan (Priority Areas of Chemistry of Coordination Space (No. 18033025) and of Super-Hierarchical Structures (No. 18039019), and 21st Century COE on Kyoto University Alliance for Chemistry), NEDO, and Kurata and Sekisui foundations for financial support.

References

1 *Organic Photovoltaics*, ed. S. S. Sun and R. S. Sariciftci, CRC, Boca Raton, 2005.
2 B. A. Gregg, *J. Phys. Chem. B*, 2003, **107**, 4688.

3 A. Hagfeldt and M. Grätzel, *Acc. Chem. Res.*, 2000, **33**, 269.
4 N. S. Lewis, *Inorg. Chem.*, 2005, **44**, 6900.
5 M. Grätzel, *J. Photochem. Photobiol., A*, 2004, **163**, 3.
6 M. Wei, Y. Konishi, H. Zhou, M. Yanagida, H. Sugihara and H. Arakawa, *J. Mater. Chem.*, 2006, **16**, 1287.
7 F. Padinger, R. S. Rittberger and N. S. Sariciftci, *Adv. Funct. Mater.*, 2003, **13**, 85.
8 M. Hiramoto, H. Fujiwara and M. Yokoyama, *Appl. Phys. Lett.*, 1991, **58**, 1062.
9 G. Yu, J. Gao, J. C. Hummelen, F. Wudl and A. J. Heeger, *Science*, 1995, **270**, 1789.
10 J. J. M. Halls, C. A. Walsh, N. C. Greenham, E. A. Marseglia, R. H. Friend, S. C. Moratti and A. B. Holmes, *Nature*, 1995, **376**, 498.
11 L. Schmidt-Mende, A. Fechtenkötter, K. Müllen, E. Moons, R. H. Friend and J. D. MacKenzie, *Science*, 2001, **293**, 1119.
12 W. U. Huynh, J. J. Dittmer and A. P. Alivisatos, *Science*, 2002, **295**, 2425.
13 M. M. Wienk, J. M. Kroon, W. J. H. Verhees, J. Knol, J. C. Hummelen, P. A. van Hal and R. A. J. Janssen, *Angew. Chem., Ind. Ed.*, 2003, **42**, 3371.
14 J. Xue, S. Uchida, B. P. Rand and S. R. Forrest, *Appl. Phys. Lett.*, 2004, **84**, 3013.
15 J. Jin, L. S. Li, Y. Li, Y. J. Zhang, X. Chen, D. Wang, S. Jiang and T. J. Li, *Langmuir*, 1999, **15**, 4565.
16 C. Luo, C. Huang, L. Gan, D. Zhou, W. Xia, Q. Zhuang, Y. Zhao and Y. Huang, *J. Phys. Chem.*, 1996, **100**, 16685.
17 W. Zhang, Y. Shi, L. Gan, C. Huang, H. Luo, D. Wu and N. Li, *J. Phys. Chem. B*, 1999, **103**, 675.
18 D. Zhou, L. Gan, C. Luo, H. Tan, C. Huang, G. Yao, X. Zhao, Z. Liu, X. Xia and B. Zhang, *J. Phys. Chem.*, 1996, **100**, 3150.
19 W. Zhang, L. Gan and C. Huang, *J. Mater. Chem.*, 1998, **8**, 1731.
20 N. V. Tkachenko, E. Vuorimaa, T. Kesti, A. S. Alekseev, A. Y. Tauber, P. H. Hynninen and H. Lemmetyinen, *J. Phys. Chem. B*, 2000, **104**, 6371.
21 N. V. Tkachenko, V. Vehmanen, J.-P. Nikkanen, H. Yamada, H. Imahori, S. Fukuzumi and H. Lemmetyinen, *Chem. Phys. Lett.*, 2002, **366**, 245.
22 T. Vuorinen, K. Kaunisto, N. V. Tkachenko, A. Efimov and H. Lemmetyinen, *Langmuir*, 2005, **21**, 5383.
23 H. Imahori, T. Azuma, S. Ozawa, H. Yamada, K. Ushida, A. Ajavakom, H. Norieda and Y. Sakata, *Chem. Commun.*, 1999, 557.
24 H. Imahori, T. Azuma, A. Ajavakom, H. Norieda, H. Yamada and Y. Sakata, *J. Phys. Chem. B*, 1999, **103**, 7233.
25 O. Enger, F. Nuesch, M. Fibbioli, L. Echegoyen, E. Pretsch and F. Diederich, *J. Mater. Chem.*, 2000, **10**, 2231.
26 T. Akiyama, H. Imahori, A. Ajavakom and Y. Sakata, *Chem. Lett.*, 1996, 907.
27 H. Imahori, S. Ozawa, K. Ushida, M. Takahashi, T. Azuma, A. Ajavakom, T. Akiyama, M. Hasegawa, S. Taniguchi, T. Okada and Y. Sakata, *Bull. Chem. Soc. Jpn.*, 1999, **72**, 485.
28 H. Yamada, H. Imahori and S. Fukuzumi, *J. Mater. Chem.*, 2002, **12**, 2034.
29 D. Hirayama, T. Yamashiro, K. Takimiya, Y. Aso, T. Otsubo, H. Norieda, H. Imahori and Y. Sakata, *Chem. Lett.*, 2000, 570.
30 D. Hirayama, K. Takimiya, Y. Aso, T. Otsubo, T. Hasobe, H. Yamada, H. Imahori, S. Fukuzumi and Y. Sakata, *J. Am. Chem. Soc.*, 2002, **124**, 532.
31 H. Imahori, H. Yamada, S. Ozawa, K. Ushida and Y. Sakata, *Chem. Commun.*, 1999, 1165.
32 H. Imahori, H. Yamada, Y. Nishimura, I. Yamazaki and Y. Sakata, *J. Phys. Chem. B*, 2000, **104**, 2099.
33 H. Imahori, H. Norieda, H. Yamada, Y. Nishimura, I. Yamazaki, Y. Sakata and S. Fukuzumi, *J. Am. Chem. Soc.*, 2001, **123**, 100.
34 S. Saha, L. E. Johansson, A. H. Flood, H.-R. Tseng, J. I. Zink and J. F. Stoddart, *Small*, 2005, **1**, 87.
35 S. Saha, E. Johansson, A. H. Flood, H.-R. Tseng, J. I. Zink and J. F. Stoddart, *Chem.—Eur. J.*, 2005, **11**, 6846.
36 K.-S. Kim, M.-S. Kang, H. Ma and A. K.-Y. Jen, *Chem. Mater.*, 2004, **16**, 5058.
37 M. Morisue, S. Yamatsu, N. Haruta and Y. Kobuke, *Chem.—Eur. J.*, 2005, **11**, 5563.
38 H. Yamada, H. Imahori, Y. Nishimura, I. Yamazaki and S. Fukuzumi, *Adv. Mater.*, 2002, **14**, 892.
39 H. Yamada, H. Imahori, Y. Nishimura, I. Yamazaki, T. K. Ahn, S. K. Kim, D. Kim and S. Fukuzumi, *J. Am. Chem. Soc.*, 2003, **125**, 9129.
40 H. Imahori, M. Kimura, K. Hosomizu and S. Fukuzumi, *J. Photochem. Photobiol., A*, 2004, **166**, 57.
41 H. Imahori, M. Kimura, K. Hosomizu, T. Sato, T. K. Ahn, S. K. Kim, D. Kim, Y. Nishimura, I. Yamazaki, Y. Araki, O. Ito and S. Fukuzumi, *Chem.—Eur. J.*, 2004, **10**, 5111.
42 V. Chukharev, T. Vuorinen, A. Efimov, N. V. Tkachenko, M. Kimura, S. Fukuzumi, H. Imahori and H. Lemmetyinen, *Langmuir*, 2005, **21**, 6385.
43 M. Isosomppi, N. V. Tkachenko, A. Efimov, K. Kaunisto, K. Hosomizu, H. Imahori and H. Lemmetyinen, *J. Mater. Chem.*, 2005, **15**, 4546.
44 Y.-J. Cho, T. K. Ahn, H. Song, K. S. Kim, C. Y. Lee, W. S. Seo, K. Lee, S. K. Kim, D. Kim and J. T. Park, *J. Am. Chem. Soc.*, 2005, **127**, 2380.
45 A. Ikeda, T. Hatano, S. Shinkai, T. Akiyama and S. Yamada, *J. Am. Chem. Soc.*, 2001, **123**, 4855.
46 T. Konishi, A. Ikeda and S. Shinkai, *Tetrahedron*, 2005, **61**, 4881.
47 E. Bustos, J. Manriquez, L. Echegoyen and L. A. Godínez, *Chem. Commun.*, 2005, 1613.
48 M. Lahav, V. Heleg-Shabtai, J. Wasserman, E. Katz, I. Willner, H. Durr, Y.-Z. Hu and S. H. Bossmann, *J. Am. Chem. Soc.*, 2000, **122**, 11480.
49 C. Luo, D. M. Guldi, M. Maggini, E. Menna, S. Mondini, N. A. Kotov and M. Prato, *Angew. Chem., Int. Ed.*, 2000, **39**, 3905.
50 D. M. Guldi, F. Pellarini, M. Prato, C. Granito and L. Troisi, *Nano Lett.*, 2002, **2**, 965.
51 F. B. Abdelrazzaq, R. C. Kwong and M. E. Thompson, *J. Am. Chem. Soc.*, 2002, **124**, 4796.
52 D. M. Guldi, I. Zilbermann, G. A. Anderson, K. Kordatos, M. Parato, R. Tafuro and L. Valli, *J. Mater. Chem.*, 2004, **14**, 303.
53 I. Zilbermann, G. A. Anderson, D. M. Guldi, H. Yamada, H. Imahori and S. Fukuzumi, *J. Porphyrins Phthalocyanines*, 2003, **7**, 357.
54 D. M. Guldi, I. Zilbermann, G. A. Anderson, A. Li, D. Balbinot, N. Jux, M. Hatzimarinaki, A. Hirsch and M. Prato, *Chem. Commun.*, 2004, 726.
55 D. M. Guldi, I. Zilbermann, A. Lin, M. Braun and A. Hirsch, *Chem. Commun.*, 2004, 96.
56 S. Conoci, D. M. Guldi, S. Nardis, R. Paolesse, K. Kordatos, M. Prato, G. Ricciardi, M. G. H. Vicente, I. Zilbermann and L. Valli, *Chem.—Eur. J.*, 2004, **10**, 6523.
57 D. M. Guldi and M. Prato, *Chem. Commun.*, 2004, 2517.
58 D. M. Guldi, *J. Phys. Chem. B*, 2005, **109**, 11432.
59 P. G. Hoertz and T. E. Mallouk, *Inorg. Chem.*, 2005, **44**, 6828.
60 F. Fungo, L. Otero, C. D. Borsarelli, E. N. Durantini, J. J. Silber and L. Sereno, *J. Phys. Chem. B*, 2002, **106**, 4070.
61 H. Imahori, J.-C. Liu, H. Hotta, A. Kira, T. Umeyama, Y. Matano, G. Li, S. Ye, M. Isosomppi, N. V. Tkachenko and H. Lemmetyinen, *J. Phys. Chem. B.*, 2005, **109**, 18465.
62 H. Imahori, J.-C. Liu, K. Hosomizu, T. Sato, Y. Mori, H. Hotta, Y. Matano, Y. Araki, O. Ito, N. Maruyama and S. Fujita, *Chem. Commun.*, 2004, 2066.
63 C.-H. Huang, N. D. McCenaghan, A. Kuhn, J. W. Hofstraat and D. M. Bassani, *Org. Lett.*, 2005, **7**, 3409.
64 Y. Liu, S. Xiao, H. Li, Y. Li, H. Liu, F. Lu, J. Zhuang and D. Zhu, *J. Phys. Chem. B*, 2004, **108**, 6256.
65 H. Imahori, K. Hagiwara, T. Akiyama, M. Aoki, S. Taniguchi, T. Okada, M. Shirakawa and Y. Sakata, *Chem. Phys. Lett.*, 1996, **263**, 545.
66 H. Imahori and Y. Sakata, *Adv. Mater.*, 1997, **9**, 537.
67 H. Imahori and Y. Sakata, *Eur. J. Org. Chem.*, 1999, 2445.
68 H. Imahori and S. Fukuzumi, *Adv. Mater.*, 2001, **13**, 1197.
69 H. Imahori, Y. Mori and Y. Matano, *J. Photochem. Photobiol., C*, 2003, **4**, 51.
70 H. Imahori, *Org. Biomol. Chem.*, 2004, **2**, 1425.
71 P. V. Kamat, S. Barazzouk, K. G. Thomas and S. Hotchandani, *J. Phys. Chem. B*, 2000, **104**, 4014.
72 S. Barazzouk, S. Hotchandani and P. V. Kamat, *Adv. Mater.*, 2001, **13**, 1614.

73 H. Hotta, S. Kang, T. Umeyama, Y. Matano, K. Yoshida, S. Isoda and H. Imahori, *J. Phys. Chem. B*, 2005, **109**, 5700.
74 P. K. Sudeep, B. I. Ipe, K. G. Thomas, M. V. George, S. Barazzouk, S. Hotchandani and P. V. Kamat, *Nano Lett.*, 2002, **2**, 29.
75 P. V. Kamat, M. Haria and S. Hotchandani, *J. Phys. Chem.*, 2004, **108**, 5166.
76 A. Kira, T. Umeyama, Y. Matano, K. Yoshida, S. Isoda, M. Isosomppi, N. V. Tkachenko, H. Lemmetyinen and H. Imahori, *Langmuir*, 2006, **22**, 5497.
77 T. Hasobe, H. Imahori, S. Fukuzumi and P. V. Kamat, *J. Mater. Chem.*, 2003, **13**, 2515.
78 T. Hasobe, H. Imahori, S. Fukuzumi and P. V. Kamat, *J. Phys. Chem. B*, 2003, **107**, 12105.
79 T. Hasobe, P. V. Kamat, M. A. Absalom, Y. Kashiwagi, J. Sly, M. J. Crossley, K. Hosomizu, H. Imahori and S. Fukuzumi, *J. Phys. Chem. B*, 2004, **108**, 12865.
80 P. V. Kamat, S. Barazzouk, S. Hotchandani and K. G. Thomas, *Chem.—Eur. J.*, 2000, **6**, 3914.
81 H. Imahori, T. Hasobe, H. Yamada, P. V. Kamat, S. Barazzouk, M. Fujitsuka, O. Ito and S. Fukuzumi, *Chem. Lett.*, 2001, 784.
82 K. Okamoto, T. Hasobe, N. V. Tkachenko, H. Lemmetyinen, P. V. Kamat and S. Fukuzumi, *J. Phys. Chem. A*, 2005, **109**, 4662.
83 T. Hasobe, S. Hattori, H. Kotani, K. Ohkubo, K. Hosomizu, H. Imahori, P. V. Kamat and S. Fukuzumi, *Org. Lett.*, 2004, **6**, 3103.
84 T. Hasobe, S. Hattori, P. V. Kamat, Y. Wada and S. Fukuzumi, *J. Mater. Chem.*, 2005, **15**, 372.
85 S. Fukuzumi, H. Kotani, K. Ohkubo, S. Ogo, N. V. Tkachenko and H. Lemmetyinen, *J. Am. Chem. Soc.*, 2004, **126**, 1600.
86 V. Biju, S. Barazzouk, K. G. Thomas, M. V. George and P. V. Kamat, *Langmuir*, 2001, **17**, 2930.
87 H. Imahori, *J. Phys. Chem. B*, 2004, **108**, 6130.
88 H. Imahori and S. Fukuuzmi, *Adv. Funct. Mater.*, 2004, **14**, 525.
89 H. Imahori, K. Hagiwara, M. Aoki, T. Akiyama, S. Taniguchi, T. Okada, M. Shirakawa and Y. Sakata, *J. Am. Chem. Soc.*, 1996, **118**, 11771.
90 N. V. Tkachenko, C. Guenther, H. Imahori, K. Tamaki, Y. Sakata, S. Fukuzumi and H. Lemmetyinen, *Chem. Phys. Lett.*, 2000, **326**, 344.
91 H. Imahori, N. V. Tkachenko, V. Vehmanen, K. Tamaki, H. Lemmetyinen, Y. Sakata and S. Fukuzumi, *J. Phys. Chem. A*, 2001, **105**, 1750.
92 V. Vehmanen, N. V. Tkachenko, H. Imahori, S. Fukuzumi and H. Lemmetyinen, *Spectrochim. Acta, Sect. A*, 2001, **57**, 2229.
93 P. D. W. Boyd and C. A. Reed, *Acc. Chem. Res.*, 2005, **38**, 235.
94 T. Hasobe, Y. Kashiwagi, M. Absalom, K. Hosomizu, M. J. Crossley, H. Imahori, P. V. Kamat and S. Fukuzumi, *Adv. Mater.*, 2004, **16**, 975.
95 T. Hasobe, P. V. Kamat, V. Troiani, N. Solladié, T. K. Ahn, S. K. Kim, D. Kim, A. Kongkanand, S. Kuwabata and S. Fukuzumi, *J. Phys. Chem. B*, 2005, **109**, 19.
96 T. Hasobe, H. Imahori, S. Fukuzumi and P. V. Kamat, *J. Am. Chem. Soc.*, 2003, **125**, 14962.
97 T. Hasobe, H. Imahori, P. V. Kamat, T. K. Ahn, S. K. Kim, D. Kim, A. Fujimoto, T. Hirakawa and S. Fukuzumi, *J. Am. Chem. Soc.*, 2005, **127**, 1216.
98 H. Imahori, A. Fujimoto, S. Kang, H. Hotta, K. Yoshida, T. Umeyama, Y. Matano and S. Isoda, *Tetrahedron*, 2006, **62**, 1955.
99 H. Imahori, A. Fujimoto, S. Kang, H. Hotta, K. Yoshida, T. Umeyama, Y. Matano and S. Isoda, *Adv. Mater.*, 2005, **17**, 1727.
100 H. Imahori, A. Fujimoto, S. Kang, H. Hotta, K. Yoshida, T. Umeyama, Y. Matano, S. Isoda, M. Isosomppi, N. V. Tkachenko and H. Lemmetyinen, *Chem.—Eur. J.*, 2005, **11**, 7265.
101 H. Imahori, K. Mitamura, T. Umeyama, K. Hosomizu, Y. Matano, K. Yoshida and S. Isoda, *Chem. Commun.*, 2006, 406.
102 H. Imahori, K. Mitamura, Y. Shibano, T. Umeyama, Y. Matano, K. Yoshida, S. Isoda, Y. Araki and O. Ito, *J. Phys. Chem. B*, 2006, **110**, 11399.
103 T. Hasobe, S. Hattori, P. V. Kamat, Y. Urano, N. Umezawa, T. Nagano and S. Fukuzumi, *Chem. Phys.*, 2005, **319**, 243.
104 T. Hasobe, S. Hattori, P. V. Kamat and S. Fukuzumi, *Tetrahedron*, 2006, **62**, 1937.
105 H. Imahori, M. Arimura, T. Hanada, Y. Nishimura, I. Yamazaki, Y. Sakata and S. Fukuzumi, *J. Am. Chem. Soc.*, 2001, **123**, 335.
106 H. Imahori, Y. Kashiwagi, Y. Endo, T. Hanada, Y. Nishimura, I. Yamazaki, Y. Araki, O. Ito and S. Fukuzumi, *Langmuir*, 2004, **20**, 73.
107 S. Kang, T. Umeyama, M. Ueda, Y. Matano, H. Hotta, K. Yoshida, S. Isoda and H. Imahori, *Adv. Mater.*, 2006, **18**, DOI: 10.1002/adma.200600312.
108 S. Barazzouk, S. Hotchandani, K. Vinodgopal and P. V. Kamat, *J. Phys. Chem. B*, 2004, **108**, 17015.
109 T. Hasobe, S. Fukuzumi and P. V. Kamat, *Angew. Chem., Int. Ed.*, 2006, **45**, 755.
110 I. Robel, B. A. Bunker and P. V. Kamat, *Adv. Mater.*, 2005, **17**, 2458.